# Journal Pre-proof


Effect of tempering on the impact-abrasive and abrasive wear resistance of ultra-high strength steels

Oskari Haiko, Kati Valtonen, Antti Kaijalainen, Sampo Uusikallio, Jaakko Hannula, Tommi Liimatainen, Jukka Kömi

PII: S0043-1648(19)30830-0

DOI: https://doi.org/10.1016/j.wear.2019.203098

Reference: WEA 203098

To appear in: *Wear*

Received Date: 17 May 2019

Revised Date: 18 October 2019

Accepted Date: 19 October 2019

Please cite this article as: O. Haiko, K. Valtonen, A. Kaijalainen, S. Uusikallio, J. Hannula, T. Liimatainen, J. Kömi, Effect of tempering on the impact-abrasive and abrasive wear resistance of ultra-high strength steels, *Wear* (2019), doi: https://doi.org/10.1016/j.wear.2019.203098.

# Effect of tempering on the impact-abrasive and abrasive wear resistance of ultra-high strength steels

Oskari Haiko[1*], Kati Valtonen[2], Antti Kaijalainen[1], Sampo Uusikallio[1], Jaakko Hannula[1], Tommi Liimatainen[3], Jukka Kömi[1]

[1] Materials and Mechanical Engineering, Centre for Advanced Steels Research, University of Oulu, Finland
[2], Materials Science and Environmental Engineering, Tampere Wear Center, Tampere University, Finland
[3] SSAB Europe, Raahe Works, Finland

[*]Corresponding author. Email address: oskari.haiko@oulu.fi, (O. Haiko)

Keywords: Wear testing; steel; abrasion; tempering; impact-abrasion

Abstract

Tempering is an essential part in the fabrication of ultra-high strength steels and it is also widely applied in the processing of wear-resistant steels. In this paper, the effects of different tempering temperatures on the impact-abrasive wear properties of martensitic ultra-high strength steels were studied. A novel press-hardening steel with carbon content of 0.4 wt.% was received in hot-rolled condition and further austenitized, water-quenched and tempered for two hours at different temperatures (150–400 °C). Tensile strength values up to 2200 MPa and hardness exceeding 650 HV were measured. Wear testing was done with impact-abrasive impeller-tumbler and abrasive dry-pot application-oriented test methods simulating mining and mineral handling environments. A laboratory rolled 600 HB steel and a commercial 500 HB grade wear-resistant steel were included for comparison. The wear surfaces and cross-sections of the samples were thoroughly characterized. Both testing methods produced highly deformed surface layers and strong work-hardening. Wear performance was mainly controlled by the initial hardness of the steels, but differences were found in the highly work-hardened surfaces of the steels.

## 1. Introduction

Ultra-high strength steels are commonly utilized in different industrial sectors ranging from mining and mineral handling to agriculture and farming operations. Harsh environments with heavy abrasive conditions require materials with extreme wear resistance. White cast irons, Hadfield (high-manganese) alloys, and numerous different steel grades are often used in the various applications found in the aforementioned sectors. Wear-resistant steels are perhaps the most used materials in abrasive and, to some extent, in impact-abrasive conditions. The cost-efficient production of modern ultra-high strength steels make them a very competitive option for the wear-applications.

Commercial wear-resistant steels are often provided in different hardness grades, usually marketed with the Brinell hardness number indicating the hardness of the steel. In the market, these steels can be found with hardness values up to 700 HB/770 HV. Apart from tool steels and other carbide-reinforced microstructures, the highest hardness among steels are generally found with martensitic steels, though also ultra-high strength bainitic steels are quite intensively studied [1–6]. Traditionally, it has been known that carbon steels may reach maximum hardness of around 800 to

900 HV [7]. However, the producibility and usability of plain carbon steels within this hardness range are not as good as lower hardness grade steels.

The carbon content for the commercial, alloyed martensitic steels with hardness above 600 HV is typically 0.4 to 0.6 wt.% and ultimate strength levels go up to 2500 MPa. Some well-known steels in this category are AISI 43xx series, 51Cr4V, and many boron steel grades. The toughness and elongation properties are usually limited, and alloying content is also relatively high to ensure full hardenability and to avoid total loss of impact toughness properties. Therefore, different processing routes and heat treatments are used in the production of high-hardness steels.

Quenching and tempering are widely utilized in the manufacturing process of the ultra-high strength, high-hardness martensitic steels. Nowadays, also the novel direct quenching (DQ) with thermomechanically controlled processing (TMCP) are used to fabricate ultra-high strength steels without need for subsequent tempering treatments or heavy alloying [8–10]. However, the conventional reheating, quenching and tempering route is still the main method for producing many high-hardness steels with medium carbon content. The adjustment of austenization temperature, quenching rate, and tempering parameters is essential when targeting for desired mechanical properties and usability. Quench and press hardening methods are also utilized, especially in the production of more complex-shaped parts, such as cutting blades and chisel ploughs. The quenching media in the process can be water, different aqueous solutions, or oil depending on the alloying content and whether quench cracking is expected.

Tempering, in general, is a very common method to improve the mechanical properties of steels [11,12]. In most cases, the quenched ultra-high strength steels require tempering treatments to increase the toughness properties. Low-temperature tempering at temperature range of 150 to 250 °C is commonly used as it does not cause drastic decrease of hardness nor strength. The high hardness should be retained in order to maintain good wear resistance, specifically against abrasion. Thus, the effect of tempering on the wear resistance is of great interest. Some examples of studies conducted on the topic can be found by Trevisiol et al. [13], Wen et al. [14], and Wei et al. [15]. However, the wear tests have been typically done using pin-on-disc or another similar very simplified device. Therefore, the aim of the current study was to complete wear tests with more application-oriented testing methods in order to characterize the differences in wear behavior of tempered and quenched steels.

## 2. Materials and methods

Experimental steel sheet material with 10 mm thickness (C43) was received in hot-rolled condition. Test plates (300 mm x 250 mm) were cut from the heavy sheet to be heat treated in laboratory furnace. Plates were heated to austenitization temperature of 980 °C and held for 40 min, which was followed by quenching in water with cooling rate of approximately 80 °C/s. Different tempering treatments were then applied: 2 hours at 150, 200, 300, or 400 °C. Hot-rolled condition (HR) and water-quenched (WQ) samples with no tempering were also included in the testing.

In addition to the C43 steel, a commercial wear resistant steel (abbreviated C30) and a laboratory rolled 600 HB hardness steel (C35) were tested for comparison of mechanical properties and wear characteristics. The direct-quenched C30 steel was received as 12 mm thick heavy plate. The C35 steel was hot-rolled in the laboratory mill. The steel was originally cast by OCAS, Belgium. Before hot rolling, the C35 laboratory scale cast was cut to ingots with dimensions of 140 mm x 80 mm x 60 mm. The ingots were then annealed at 1200 °C for 2 hours and hot rolled from the initial 60 mm thickness to 12 mm thick plates with six passes to produce samples for testing. The finish rolling

temperature was 960–980 °C and the plates were direct-quenched to a water tank. The chemical compositions for the tested steels are presented in Table 1. Composition for C43 was provided by the manufacturer and the C35 by OCAS, Belgium. The presented C30 composition is from a product sheet.

**Table 1.** Chemical compositions of the tested steels (wt.%, balance Fe).

| Material | C | Si | Mn | Al | Cr | Mo | Ni |
|---|---|---|---|---|---|---|---|
| C30* | 0.30 | 0.80 | 1.70 | - | 1.50 | 0.50 | 1.0 |
| C35 | 0.35 | 0.25 | 0.51 | 0.033 | 0.77 | 0.15 | 2.0 |
| C43 | 0.43 | 0.20 | 0.25 | 0.035 | 0.05 | 0.69 | 0.05 |

**Nominal composition, from product brochure.*

Material characterization was done with optical, laser scanning confocal (Keyence VK-X200) and field-emission scanning electron microscopes (Zeiss Sigma FESEM). Microstructures and worn sample cross-sections were polished and etched with 2 % Nital. Prior austenite grain sizes (PAGS) were determined from picric acid etched samples for planar sections using calculation tool developed by Seppälä et al. [16]. The calculations were based on linear intercept method by Sellars and Higginson [17]. Surface profile roughness values $R_a$ (arithmetic mean roughness) and $R_z$ (root mean square height) were measured using the laser scanning confocal microscope. The surface roughness measurements were based on the ISO 4287-1997 standard. Retained austenite content was measured with X-ray diffraction (XRD) method using Rikagu SmartLab 9 kW X-ray diffractometer with cobalt $K_\alpha$ radiation. Analysis of the X-ray data was done with PDXL2 software and Rietveld's whole powder fitting method. The $R_{wp}$ values were less than four for all fittings.

Tensile tests included three samples for each material variant with the reduced sample section of 10 mm x 20 mm x 120 mm. Samples were cut longitudinal to the rolling direction. MTS-810 universal servohydraulic testing machine was used for the tensile testing. Impact toughness was measured with Charpy-V method according to standard ISO 148-1 for transverse 7.5 mm x 10 mm x 55 mm samples. Three impact toughness specimens were tested at room temperature (RT) and at -40 °C for each material variant. Hardness testing through the thickness was conducted with Struers Duramin A-300 tester using Vickers HV10 method with a minimum of seven indentations per sample. Microhardness values were measured using CSM Instruments MHT-Z-AE microhardness tester. The applied force was 0.5 N and a minimum of five indentations were measured per sample.

Wear testing was done in Tampere Wear Center (TWC) at Tampere University. Two in-house application-oriented wear testing devices were selected for the testing: impeller-tumbler and dry-pot tester. The impeller-tumbler [18] is designed to cause impact-abrasive wear by freely moving abrasives. The impeller-tumbler has three samples attached to a sample holder acting as the fast-rotating impeller while the outer rim (tumbler) rotates slowly to lift the abrasives (Fig. 1a). The rotation direction is the same for the impeller and tumbler. In the current tests, the rotation speed for the impeller was 700 rpm and 30 rpm for the tumbler. The test time was 60 min, which was preceded by one 15-min period to reach steady-state wear. Three samples at a time were tested during the testing time and one of the samples was always a reference sample for monitoring the reliability of the tests. The impeller-tumbler sample dimensions were 75 mm x 25 mm x 8 mm. Gravel, crushed and sieved to 10–12 mm size distribution, used in the tests was granite from Kuru quarry, Finland. The gravel batch (900 g) was replaced every 15 min during the testing to have fresh and sharp abrasives at present. The samples were attached to the holder in 60° angle to normal. Possible distortions caused by the sample holder were minimized by switching the samples between the three holder slots for every 15-min test period, i.e. all samples were tested in all the

three sample holder slots. The samples were weighed prior and after to the testing, and between every 15-min test period.

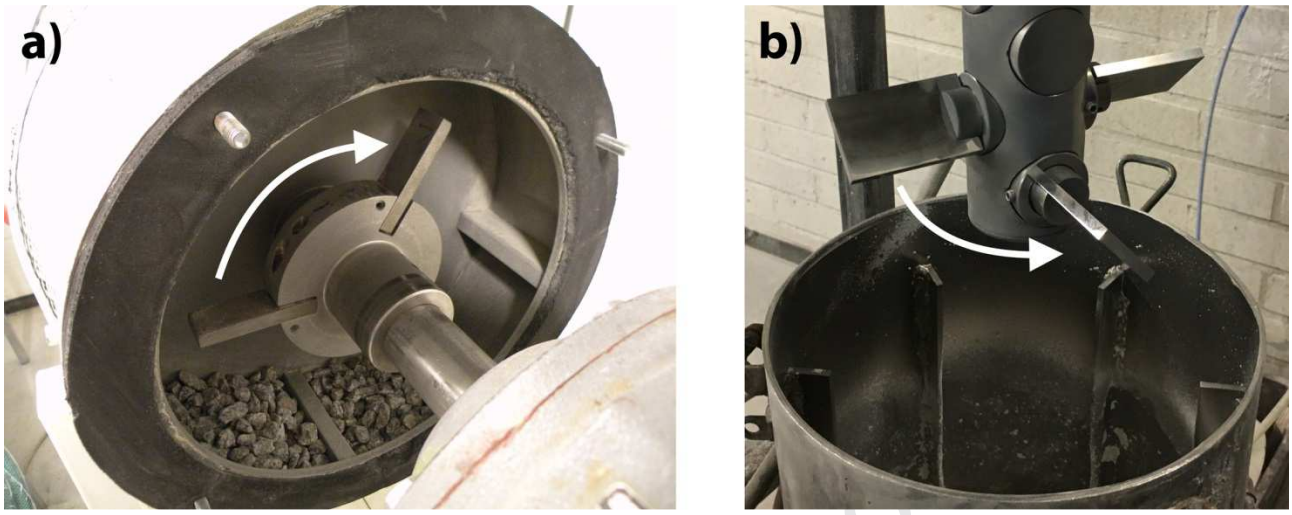


**Fig. 1.** a) Impeller-tumbler impact-abrasive tester with three samples (fitted with 90° sample holder) and b) dry-pot tester with four samples fitted in +45° angle. Rotating direction marked with arrow.

The dry-pot testing device is a pin-mill type tester which can be used with slurry [19–21] or with dry abrasive gravel bed [3,22,23]; the latter was selected for the current tests. Fig. 1b presents the tester that consists of a shaft with sample holders and a steel pot. The shaft is rotated inside the pot filled with abrasives at 250 rpm, which produces 2.5 m/s speed at the tip of the samples. Four samples were tested at each testing position and one sample was always as a reference material for monitoring the test. The total test time was 240 minutes, which included four 60 min periods. For every test period, the samples were weighed, the gravel batch was replaced, and the position of the samples was changed. Due to the nature of the dry-pot method, the gravel is more densely packed on the bottom of the device causing more severe wear in the two lowest sample positions. This was taken into account by rotating the samples between positions and reversing sample order for the second round of test samples. The gravel was Kuru granite sieved to 8–10 mm size distribution. Every 60 min test period included 9000 g of granite and 1350 g of 100–600 µm quartzite (Nilsiä quarry, Finland). The fine quartzite was used in the bottom of the test pot chamber to prevent the granite from descending under the shaft head. Samples were attached in a +45° angle to the normal and sample dimensions were 64 mm x 40 mm x 6 mm. Two samples of each material variant were tested in both wear test devices. The typical reported standard deviation for the impeller-tumbler results was under 3 % [18] and under 4 % for the dry-pot tests [23], when granite was used as an abrasive.

## 3. Results and discussion

### 3.1. Microstructures of the studied steels

The studied steels consisted of different degrees of autotempered or tempered martensite with the exception of the original hot-rolled (HR) variant of C43, which had banded ferritic-pearlitic microstructure. FESEM images of the microstructures taken at quarter depth of the sample are shown in Fig. 2. The increasing tempering temperature had a notable effect on the amount of precipitates found in the C43 samples. The formation of these precipitates had already started during the quenching when autotempering occurred. Microstructure of the water-quenched C43

sample shows typical martensitic microstructure with dark, untempered martensite and white precipitates (Fig. 2b). The fraction of precipitate-rich areas increases for the low-temperature (150 and 200 °C) tempered samples and the amount of untempered, darker martensite decreases. These small precipitates are presumably transition carbides formed in the first and second stages of tempering [7,11,12]. The tempering of C43 in the higher temperatures (300 and 400 °C) resulted in cementite formation (presumably $\theta$ carbide) replacing the fine transition carbides (Figs. 2e–f). The size of the cementite carbide grows with the tempering temperature and the cementite becomes more spheroidal.

Commercial C30 steel (Fig. 2g) consists of autotempered martensite and had as much transition carbides as the two low-temperature tempered variants of the C43. Further, the C35 steel (Fig. 2h) has also martensitic microstructure with resemblance to the C43 WQ and 150 °C samples. Autotempering had occurred, however the effect appeared as not as intense as with the C30. Nevertheless, the quenched and the low-temperature tempered variants of C43, C30 and C35 exhibited distinguishable martensitic microstructures, whereas the higher tempering temperatures of the C43 (300 and 400 °C) had become more ferrite-like with cementite present.

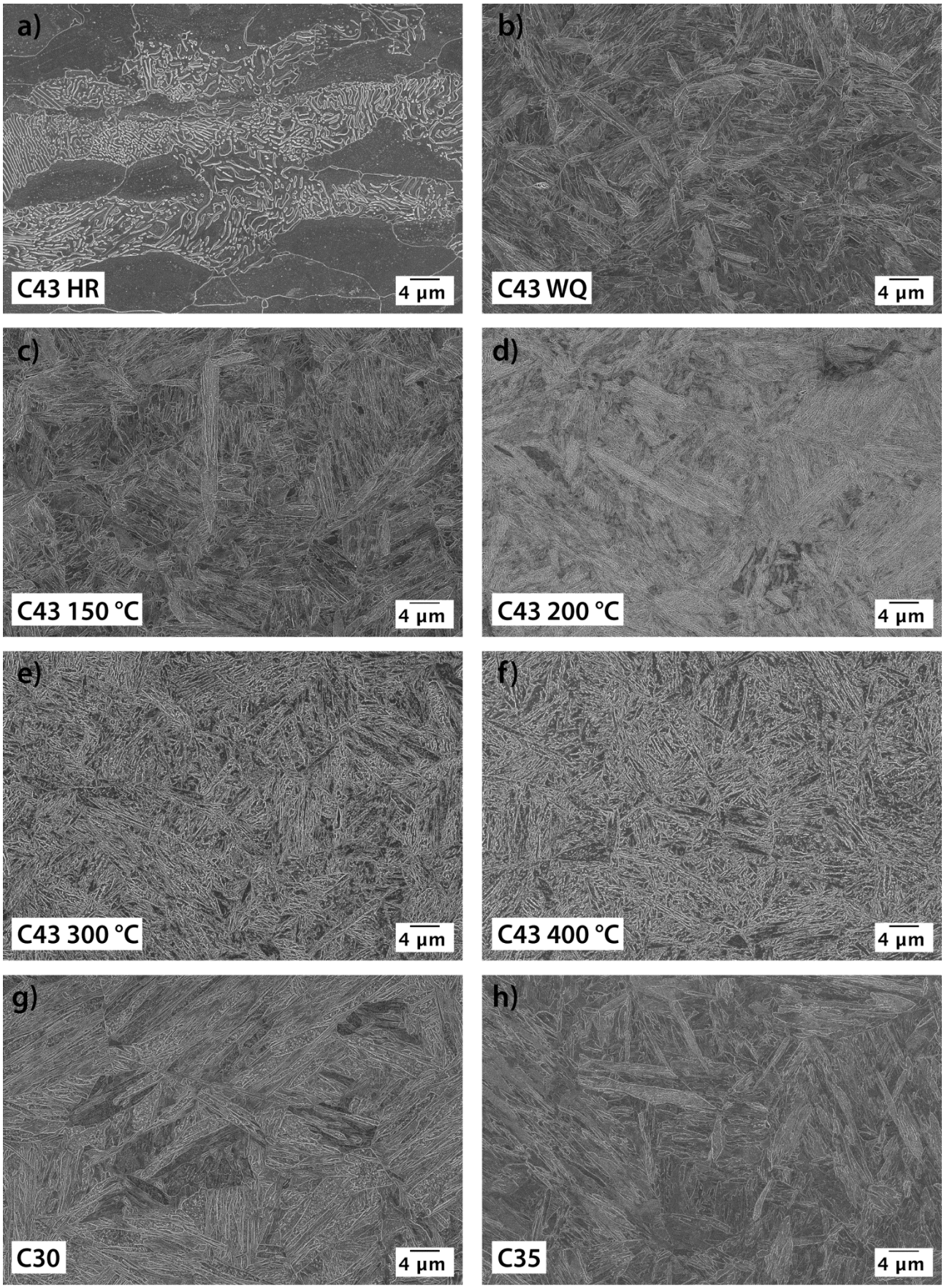


**Fig. 2.** Typical microstructures of the studied steels.

Retained austenite content was measured with XRD and the results are given in Table 2. The C43 WQ (3.6 %) and low-temperature tempered samples 150 and 200 °C (both 2.8 %) had some austenite present, but the higher tempering temperatures (300 and 400 °C) resulted in austenite decomposition. The medium carbon content of 0.43 wt.% is expected to have some retained austenite present, even with very high quenching rates. The C30 and C35 also had some retained austenite, but the values were very low (1.1 % and 1.9 %) and almost on the limit of detection accuracy.

The prior austenite grain size (PAGS) was determined for the C43 300 °C and C35 samples. The first had mean PAGS of 12.3 ± 0.6 µm with almost equiaxed grain structure. The C35 also had fairly equiaxed grain structure and mean PAGS of 20.2 ± 1.4 µm. However, the C30 proved to be very difficult to etch and to have the prior austenite grain boundaries visible and only a rough estimate of 20 µm PAGS could be given.

### 3.2. Mechanical properties

The mechanical properties of the tested steels are given in Table 2, including 0.2 % offset yield strength ($R_{p0.2}$), ultimate tensile strength ($R_m$), uniform elongation ($A_g$), bulk Vickers hardness (HV10), and impact toughness at room temperature and -40°C. The quenched and low-temperature tempered variants of C43 reached both high yield and tensile strength values, and the expected hardness level of 650 HV10 was also realized. The tempering at 150 °C did not yet cause drastic loss of strength nor hardness in comparison to the water-quenched version. The C43 WQ and 150 °C came very close to each other regarding tensile strength and bulk hardness. The yield strength was the highest for the low-tempered steels. The increase of yield strength at low tempering temperatures for martensitic steels can be attributed to the relaxation of internal stresses [24,25]. Generally, the tempering increased the yield-to-tensile strength ratio when compared to the quenched steels. The ratio increased from 0.68 (C43 WQ) to 0.92 (C43 400 °C) despite the higher tempering temperatures of 300 °C and 400 °C showing decrease of both yield and tensile strength as well as hardness values. The commercial C30 steel had quite high yield-to-tensile strength ratio (0.81), presumably due to the higher degree of autotempering, whereas the C35 steel showed ratio of 0.67, similar to the C43 WQ. Hot-rolled (HR) C43 variant had significantly lower strength, hardness and impact toughness properties, as expected for the ferritic-pearlitic microstructure.

**Table 2.** Mechanical properties with standard deviations and retained austenite content of the tested steels.

| Material | $R_{p0.2}$ [MPa] | $R_m$ [MPa] | $A_g$ [%] | Hardness HV10 [kgf/mm$^2$] | Charpy-V (RT / -40 °C) [J/cm$^2$] | Retained austenite [%] |
|---|---|---|---|---|---|---|
| C43 HR | 471 ± 24 | 711 ± 23 | 9.4 ± 0.4 | 195 ± 4 | 8 ± 0 / 5 ± 0 | - |
| C43 WQ | 1528 ± 13 | 2233 ± 9 | 5.5 ± 0.3 | 653 ± 16 | 18 ± 5 / 14 ± 2 | 3.6 |
| C43 150 °C | 1606 ± 22 | 2168 ± 28 | 5.1 ± 0.4 | 668 ± 15 | 25 ± 2 / 20 ± 3 | 2.8 |
| C43 200 °C | 1616 ± 13 | 1997 ± 15 | 4.1 ± 0.2 | 622 ± 11 | 31 ± 2 / 28 ± 2 | 2.8 |
| C43 300 °C | 1482 ± 13 | 1667 ± 14 | 3.0 ± 0.2 | 493 ± 11 | 31± 1 / 26 ± 3 | - |
| C43 400 °C | 1330 ± 2 | 1445 ± 2 | 3.0 ± 0.2 | 417 ± 11 | 43 ± 2 / 24 ± 6 | - |
| C30 | 1251 ± 10 | 1552 ± 10 | 4.4 ± 0.2 | 482 ± 10 | 57 ± 3 / 37 ± 4 | 1.1 |
| C35* | 1429 ± 9 | 2120 ± 10 | 5.3 ± 0.4 | 597 ± 9 | 19 ± 1 / 14 ± 1 | 1.9 |

*Only two tensile test samples were tested due to material restriction.

The impact toughness was measured with the standardized Charpy-V notch sample testing at two temperatures. The measured joules were directly converted proportionally to J/cm$^2$. Low-temperature testing at -40 °C showed that the tempering range of 150 to 200 °C improves the impact toughness over the quenched condition for C43. Temper martensite embrittlement (TME) [26,27] presumably caused the impact toughness to decrease with the C43 300 and 400 °C variants, though the absolute increase of impact toughness energies was low and within deviation. XRD measurements also confirmed that the decomposition of austenite had taken place for the tempering temperatures of 300 and 400 °C, which is one of the major causes for the TME. However, it can be seen that the average impact energy at room temperature testing increased sharply for the C43 400 °C. The C43 WQ had impact energies close to the C35 steel. In contrast to the higher carbon content steels, the C30 had quite good Charpy-V test results and decent impact toughness even at -40 °C, while still having tensile strength above 1500 MPa and hardness of nearly 500 HV10. The lower carbon content and thermomechanical controlled processing with the direct quenching can be considered the main reasons for the enhanced impact toughness properties of the C30. Uniform elongation values were limited for all the tested steels, except for the C43 HR variant.

### 3.3. Wear test results

#### 3.3.1. Mass loss

Wear test results are listed Table 3. Although the impeller-tumbler testing in general did not cause excessive mass loss during the 60 min test time, the test results had a clear linear correlation with the initial hardness (Fig. 3a). The best performance was found with the C43 WQ and C43 150 °C, which both had mass loss less than 0.160 g. No significant difference in wear performance could be observed for the C43 tempered at 200 °C and the direct-quenched C35 with similar hardness values. The C43 300 °C and C30 also showed nearly the same mass loss for the hardness of just below 500 HV10. The C43 400 °C had higher mass loss and also lower hardness than any of the previously discussed steels. However, the C43 400 °C also showed the highest deviation of mass loss (7.5 %) despite no higher deviation of the initial hardness values (2.6 %). The C43 HR with the lowest initial hardness had almost double the mass loss compared to the best performing samples. The initial hardness was the main factor controlling the wear resistance in the impeller-tumbler tests. The deviation of mass loss in the impeller-tumbler tests for all samples was less than 3 %, when excluding the aforementioned C43 400 °C.

The dry-pot testing resulted in similar results as the impeller-tumbler testing in terms of wear resistance (Fig. 3b). However, the absolute mass losses were higher for the dry-pot testing, leading up to 2.3 g of mass loss, which was almost ten times more than in the impeller-tumbler testing while the test time was only four times longer. The least worn samples were the C43 WQ and C43 150 °C but now there was slightly more difference between the two when compared to the impeller-tumbler testing. The most worn sample was C43 400 °C. Unfortunately, the C43 HR sample holder got loose during the testing and hence the results were discarded as unreliable. The average deviation for the mass loss of dry-pot tested samples was 2.3 %.

**Table 3.** Hardness values and wear test results for impeller-tumbler and dry-pot testing.

| Material | Hardness HV10 [kgf/mm$^2$] | Mass loss impeller-tumbler [g] | Mass loss dry-pot [g] |
|---|---|---|---|
| C43 HR | 195 ± 4 | 0.318 ± 0.001 | - |
| C43 WQ | 653 ± 16 | 0.158 ± 0.002 | 1.358 ± 0.016 |
| C43 150 °C | 668 ± 15 | 0.159 ± 0.001 | 1.406 ± 0.084 |
| C43 200 °C | 622 ± 11 | 0.178 ± 0.002 | 1.494 ± 0.021 |
| C43 300 °C | 493 ± 11 | 0.222 ± 0.004 | 1.952 ± 0.009 |
| C43 400 °C | 417 ± 11 | 0.247 ± 0.019 | 2.280 ± 0.079 |
| C30 | 482 ± 10 | 0.220 ± 0.006 | 1.934 ± 0.066 |
| C35 | 597 ± 9 | 0.179 ± 0.001 | 1.469 ± 0.003 |

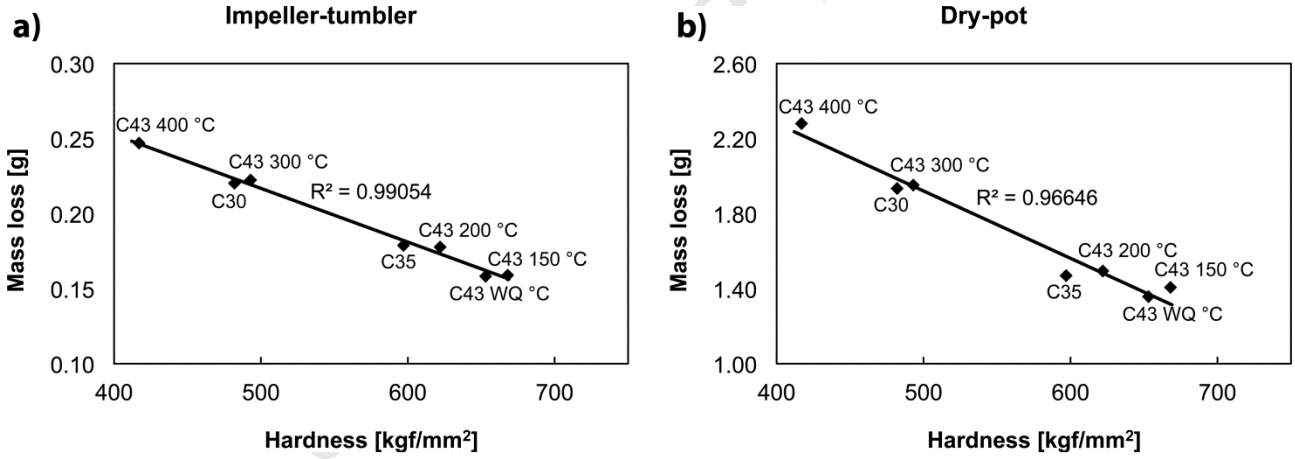


**Fig. 3.** Impeller-tumbler (a) and dry-pot (b) test results plotted on hardness vs mass loss chart (C43 HR excluded).

The wear performance in these impact-abrasive and abrasive tests were measured by mass loss, and unsurprisingly the hardness was the major factor regarding the wear resistance. It is evident that the correlation between the initial hardness and mass loss was very strong in the current tests as seen in Fig 3. This was also seen in previous tests [28,29]: the increasing hardness improves the wear resistance in abrasive conditions when similar microstructures are tested. No clear difference could be seen with the samples that had similar hardness level but differences in other mechanical properties. The direct-quenched/water-quenched samples had minor advantage in almost all hardness levels. The C43 WQ outperformed the C43 150 °C marginally in both tests, as so did the C35 over the C43 200 °C in dry-pot testing. C30 also had lower mass loss in both tests over the C43 300 °C. However, it is rather difficult to draw conclusions whether a direct-quenched or reaustenitized and water-quenched steel performs better over a quenched and tempered steel when the hardness level is the same. Though, the current results could be an indication of quenched martensitic microstructure having some advantage over tempered structure in terms of abrasive

wear resistance. More prominent differences have been discovered, for example by Ojala et al. [30], when testing martensitic steels with similar hardness level.

The cumulative mass loss during testing did not show any great differences for the steels in the impeller-tumbler testing. The samples were weighed every 15 minutes to see if any possible work hardening would have effect on the wear resistance. However, the wear rates were quite linear for all the steels throughout the 60-min test time and none of the samples showed clear linear increase or decrease of the wear rate. Substantially longer test duration might have provided more information about the work hardening or changes in the wear rate, as discussed by Ratia et al. [31] and Wilson and Hawk [32].

The dry-pot method, on the other hand, provided some interesting results in terms of the wear rate. The device sample holders are placed on the rotating shaft on different levels and this causes the lowermost samples to have more severe wear. Therefore, the two samples of each material variant were tested in different order to see the possible work hardening effect on the wear rates. Fig. 4 presents the example of the cumulative mass loss for C43 300 °C. The wear rate was substantially higher for the two lowermost sample positions (B1 and B2), however eventually this did not affect the total results. In the end of the test, the samples of the same steel variant reached the same mass loss despite the wear rate differences during the test. The severity of the work hardening had no significant effect on the total mass loss when the samples were rotated through all the four positions. In other words, it did not matter in which stage the steels were subjected to more or less severe wear. Also, the test time was 240 min, which was four times more than the test time for the impeller-tumbler. This indicates that the abrasive wear was sufficient to cause the steel to wear rapidly no matter the condition of the steel surface. In both test methods, it should be borne in mind that the most severe wear and most of the mass loss is concentrated on the tip of the samples with the highest speed, as can be seen in Fig. 5a.

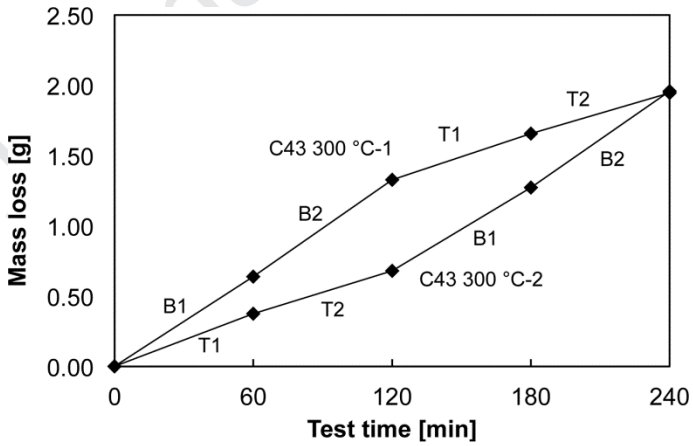


**Fig. 4.** Cumulative mass loss for the C43 300 °C samples during dry-pot testing with the sample positions marked: T (top) and B (bottom).

3.3.2. Surface roughness and granite embedment

The worn surfaces were inspected with laser scanning confocal microscope to determine the surface profile roughness values. Three measurements were conducted on each worn sample and the measured area was 3.4 mm x 2.3 mm located 10 mm from the worn tip of the sample in the middle of the sample (impeller-tumbler) or 10 mm from both edges for dry-pot samples (illustrated in Fig. 5a). The impeller-tumbler resulted in considerably higher surface roughness values compared to the

dry-pot. Earlier work by Valtonen et al. [33] showed that the nature of the impeller-tumbler is more towards impact-abrasive wear compared to the dry-pot that is an abrasive test method. The 3D-topography maps (Fig. 5b) created with the laser scanning confocal microscope also visualized the differences between the two testing methods. Fig. 6a presents the measured surface profile roughness values arithmetic mean ($R_a$) and root-mean-square height ($R_q$). Both surface roughness ($R_a$ and $R_q$) values increased almost linearly with the increasing mass loss and decreasing hardness. The connection was quite similar to the relationship between the hardness and mass loss with some small deviations. The C43 150 °C had the smoothest surface and the lowest R-values of the measured samples. For the dry-pot samples, the absolute surface roughness values were low and the differences between steels minor.

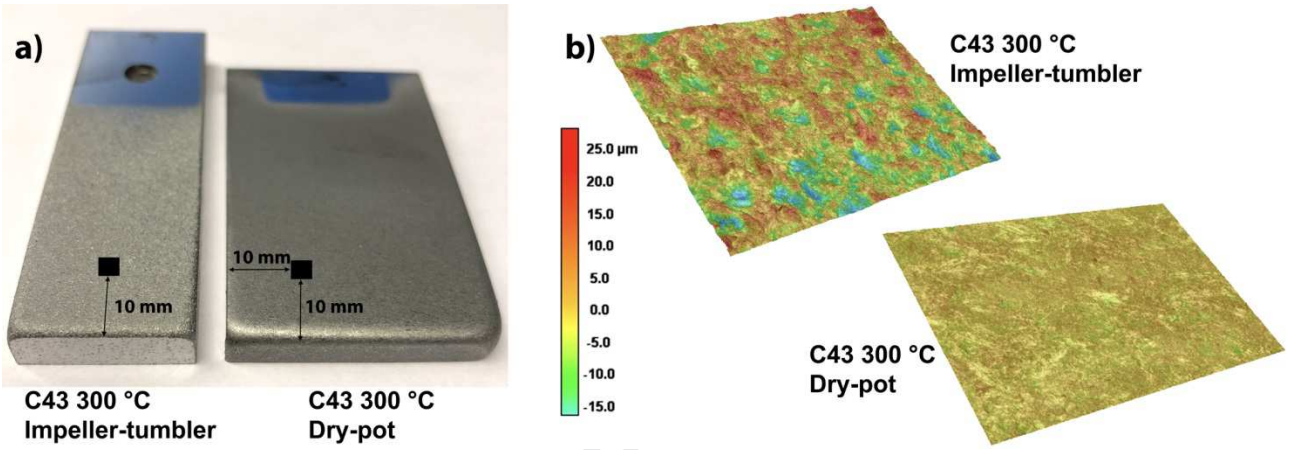


**Fig. 5.** a) Black squares present the areas measured for the surface roughness values (not in true scale), C43 300 °C samples shown and b) 3D-topography maps of the respective samples.

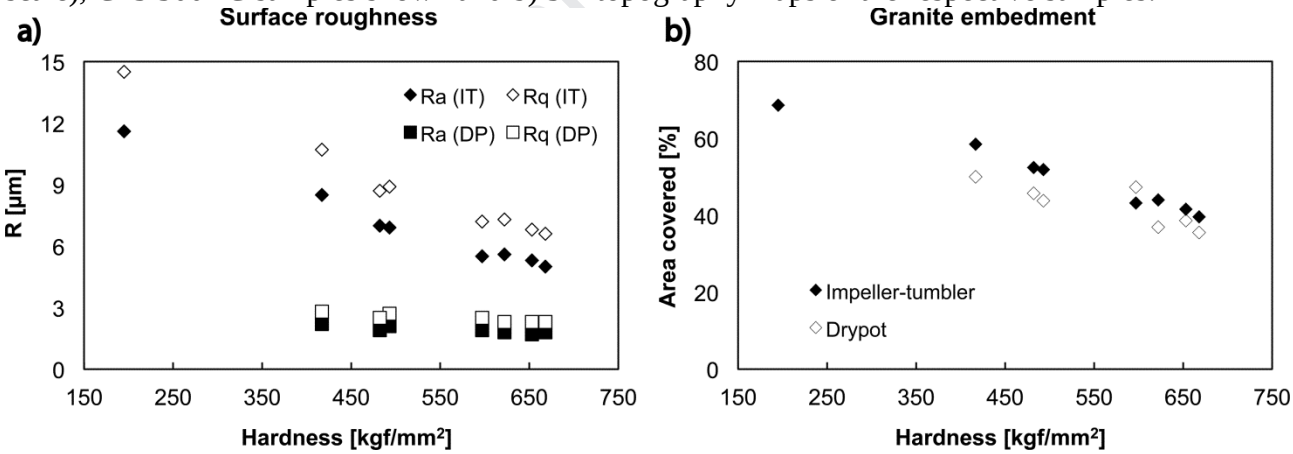


**Fig. 6.** (a) Measured surface roughness values for the impeller-tumbler testing (IT) and dry-pot testing (DP) and (b) area covered by granite in percentage for both wear testing methods.

The granite embedment and coverage in percentage were calculated from the backscatter electron (BSE) images (presented in Fig. 7). Three images were taken per each sample from 1 mm distance of the sample edge. The images were then analyzed with Fiji open-source image processing package built on the ImageJ software to calculate the area covered by the granite. The results from both test methods are plotted in Fig. 6b. The increasing hardness inhibited the penetration and therefore also the embedment of the granite particles. Thus, the lowest granite embedment was seen with the samples with the highest hardness (C43 150 °C and C43 WQ) for the impeller-tumbler samples. The granite coverage within the same hardness levels were very close to each other showing no clear differences between tempered and DQ/WQ steels.

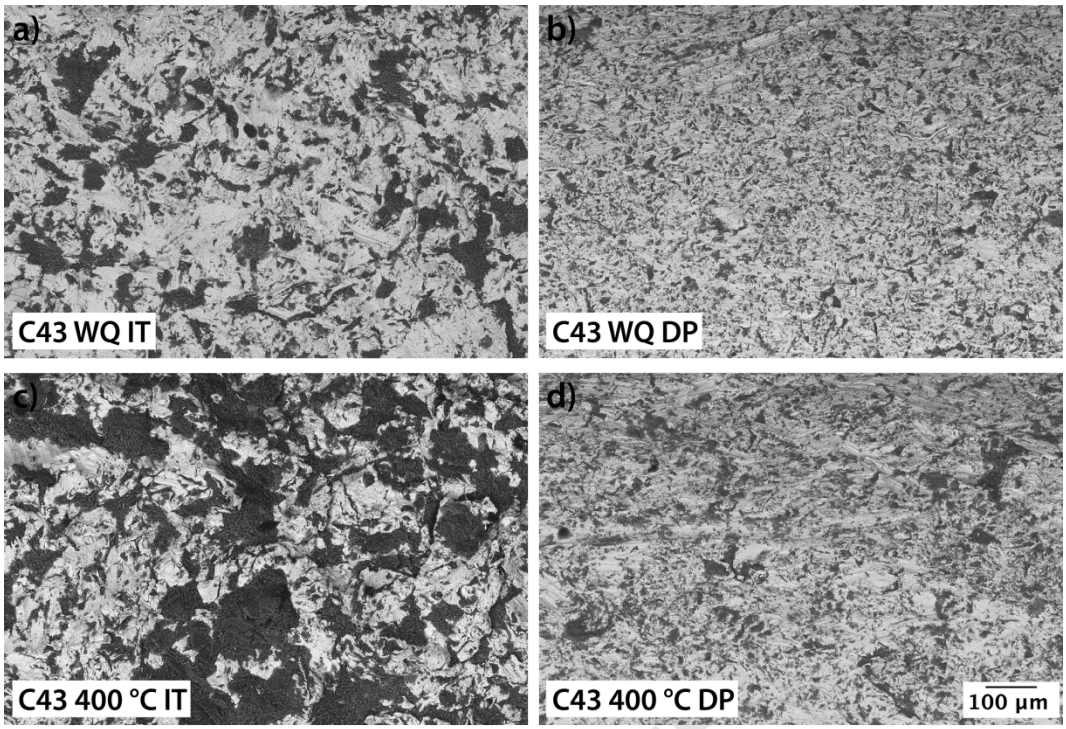


**Fig. 7.** Examples of BSE images of worn surfaces showing granite embedment (dark areas) for impeller-tumbler (IT) and dry-pot (DP) samples.

The dry-pot testing, however, did show some deviation in this regard. The C43 150 °C and C43 200 °C had similar coverage, while the hardness difference was about 50 HV. Moreover, the C35 had higher area coverage in the dry-pot testing than in the impeller-tumbler testing. It was almost as high as with the C43 400 °C. Generally, more embedded granite could be seen on the surface of the impeller-tumbler tested samples compared to the dry-pot samples (Fig. 7). In addition, the dry-pot samples seemed to be much more sensitive to the location of the area measured. In other words, the 1 mm movement from the tip of the worn sample edge was more difficult to determine compared to the impeller-tumbler samples due to more rounded edges of the dry-pot samples (see Fig. 5a). The initial idea was to measure the area coverage from the same distance of the samples for both of the test methods, but this proved to be difficult due to the more rounded edges of the dry-pot samples. Therefore, the granite embedment values for the dry-pot testing should be viewed with care. Moreover, the used image analysis method does not measure the total volume of embedded granite. Thus, the thickness of the layers and the area of the single clusters were not determined. Visually, the granite embedment areas were much bigger and thicker in impact-abrasion compared to abrasion.

### 3.3.3. Cross-sections of the worn surfaces

Cross-sectional images of the worn surfaces were taken with FESEM and laser scanning confocal microscopes. Generally, the impeller-tumbler had caused damage to a greater depth below the surface. Examples of the worn surfaces are given in Fig. 8, which shows the major differences found in the deformed surface layers of the samples, for both between the test devices and between the tested steels. The impeller-tumbler samples (Fig. 8a–c) had significantly different depth of penetration between the steels. The energy of the impacting particles has been estimated to be less than 80 mJ [29,34], but this has been sufficient to cause strong plastic deformation on the steel samples. The decreasing hardness resulted in rougher surface and higher penetration depth of the granite particles, and also the deformation of the microstructure reached deeper into the material.

The depth of the deformed layer was up to 100 µm for the C43 400 °C, whereas the hardest variants showed deformed microstructure approximately 20 to 30 µm below surface. However, the higher hardness samples had more adiabatic shear bands (ASB), and more white layer formation on the surface. The shear bands and the deformed layer appeared white when examined with optical microscope, which indicates to transformed type of shear bands and white layer [35].

The dry-pot test samples (Figs. 8d–f) had smoother surfaces, which was also seen in the surface profile roughness measurements in Figs. 5b and 6a. The cross-sections do not show as drastic differences between the steels as the impeller-tumbler samples showed. However, the deformation depth was clearly highest in the lower hardness steel and there was more embedded granite on the surface (Figs. 8d–f). Abrasion has inflicted most damage very close to the surface and the direction of the plastic flow is visible (left to right).

FESEM images of the worn surfaces show the tribolayer in detail (Figs. 9 and 10). Microploughing, microcutting and eventually surface fatigue are the wear mechanism that have taken place. A closer look of the surface shows the deformed microstructure around the embedded granite particle (Fig. 9a). Some subsurface cracks could be seen underneath the tribolayer, possibly initiated by adiabatic shear bands (Fig. 9b). The continuous impacts of the granite particles cause excessive work-hardening of the surface and may eventually result in the hardened layer to become too brittle and furthermore lead to the loss of material by delamination [36]. An example of the delamination effect can be seen with C43 300 °C impeller-tumbler sample in Fig. 10. Moreover, the very fine near nanoscale structure of the white layer and adiabatic shear bands can be seen (Fig. 9c), and the heavily deformed surface layer shows bent laths and orientated or fibered structures of the martensite (Fig. 9d). The latter phenomenon is similar to the situation found with fatigue wear caused by sliding and rolling contact [1,4]. The movement of the rocks inside the dry-pot result in the orientated and highly deformed surface layer, in which cracks initiate and propagate causing the formation of wear particles and material removal.

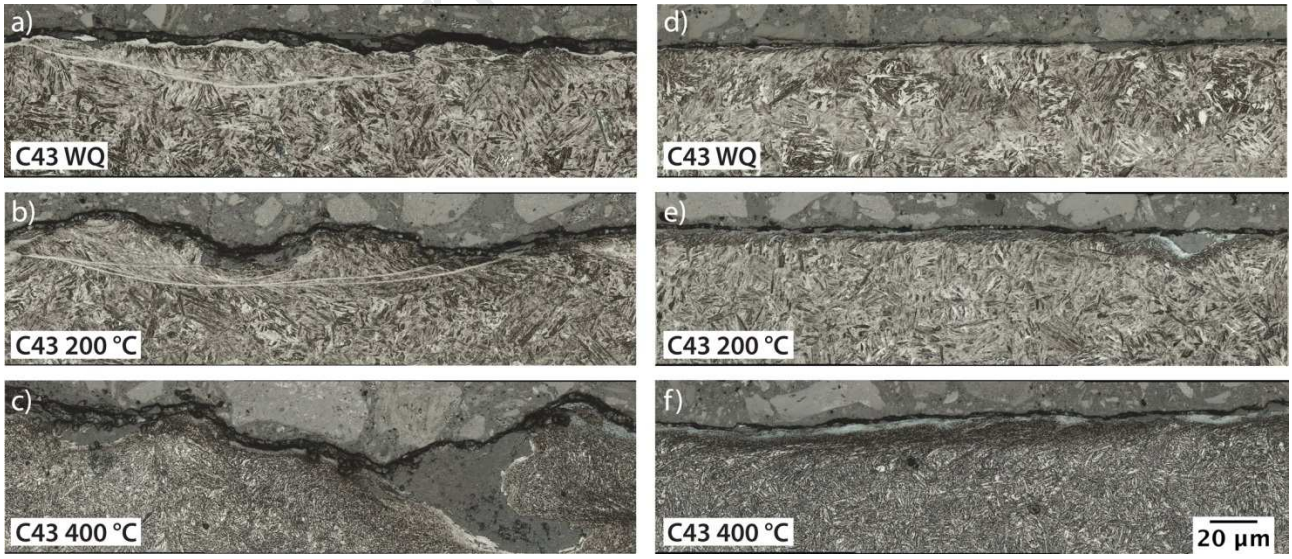


**Fig. 8.** Laser scanning confocal images of worn surfaces: (a-c) impeller-tumbler samples on left and (d-f) dry-pot samples on the right.

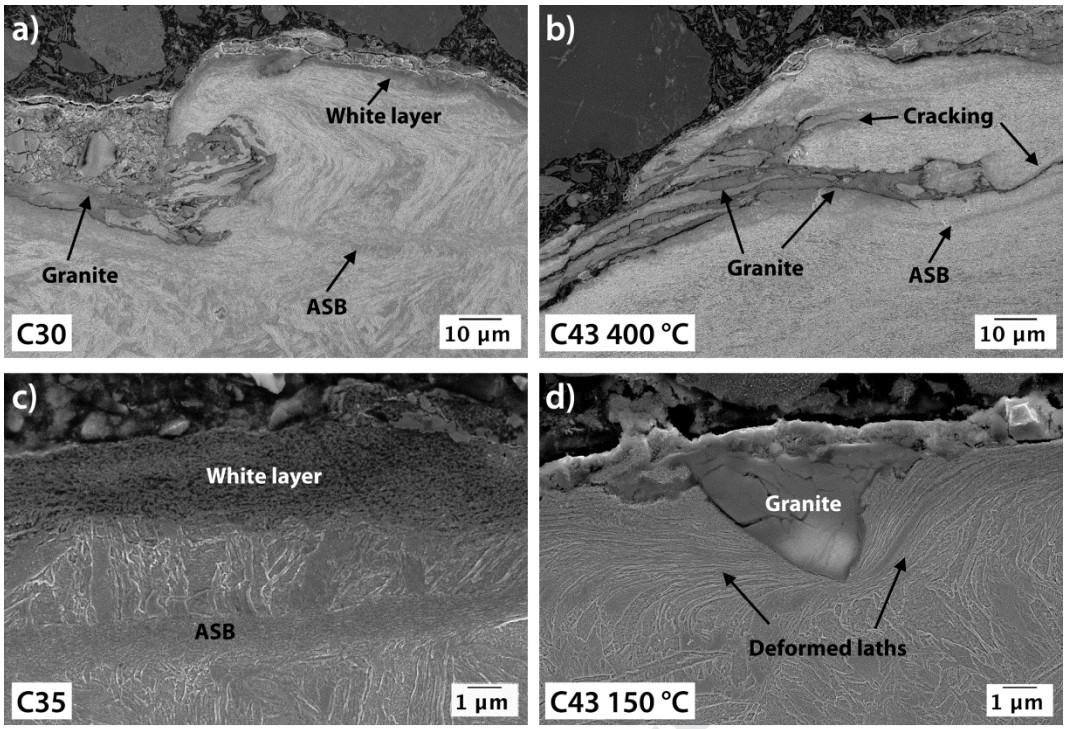


**Fig. 9.** FESEM images of worn samples: a) C30 with large granite embedment and heavily deformed microstructure (IT), b) C43 400 °C with subsurface cracks (IT), c) C35 with very fine white layer structure and shear band (IT) and d) C43 150 °C surface with surrounding deformed microstructure around the embedded granite particle (DP).

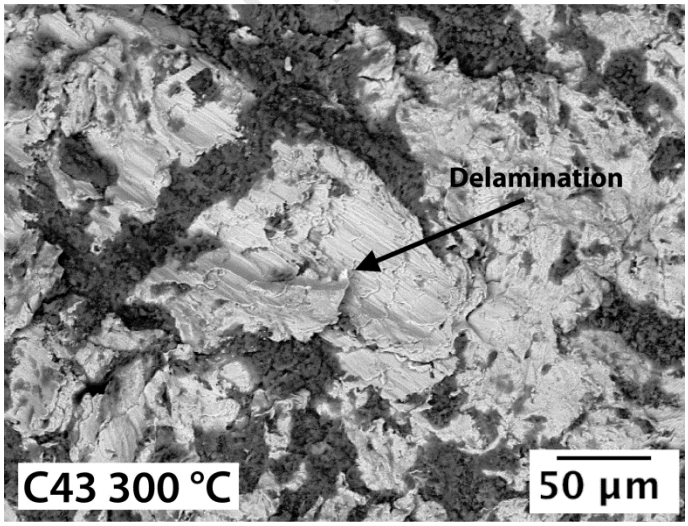


**Fig. 10.** BSE image of the worn impeller-tumbler sample with marks of delamination.

The work-hardening of the steels was studied by measuring the microhardness of the deformed microstructure as close as possible to the worn surface for the impeller-tumbler samples. The results for the microhardness measurements and the average values for the bulk hardness are given Fig. 11. All samples had increased hardness over the initial condition prior to wear testing. The C43 in water-quenched and low-temperature tempered conditions provided very similar increase in hardness with approximately 150 HV higher values over the initial hardness. The higher tempering temperatures (300 and 400 °C) showed decreased work hardening. The highest increase of hardness was measured for the direct-quenched steels C30 and C35. The deformed layer near the surface showed over 200 HV increase of hardness indicating high work-hardening capability. The hot-rolled variant (195 HV) also had highly increased surface layer hardness, but even the increased

hardness (367 HV) was still below the initial hardness of all the other steel variants tested. It should be noted that the microhardness measurements close to the worn surface with low load (0.5 N) have a high probability for errors and therefore the absolute values should be treated with care. The deviation for the measurements was high, mainly due to the highly localized deformation and different degree of work-hardening.

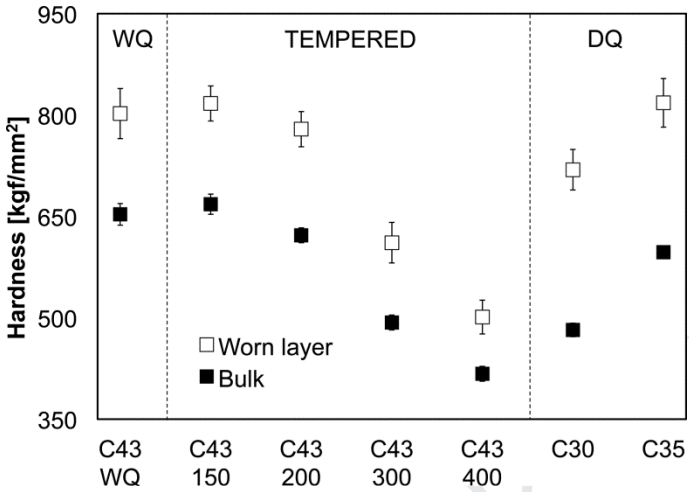


**Fig. 11.** Microhardness of the deformed layer of the impeller-tumbler samples.

3.4. Factors affecting the wear performance of quenched and tempered steels

Hardness has been shown to have a great effect on the wear performance of steels, and in this study, it was also the main controlling factor of impact-abrasive wear. By definition, hardness is the material property that resists abrasion or indentation, therefore it plays a major role in the wear resistance of steels. In the current study, tempering at 200 °C or higher temperatures led to decreased hardness and higher mass loss in wear testing. The tempered steels in general exhibited higher yield strength and improved impact toughness, but neither of these properties appeared to have an effect on the wear performance. In real world wear systems and conditions, the impact energies are notably higher than in the impeller-tumbler device, and the abrasive size can be multiple times larger, for example in mining or agricultural operations. This might lead into a more severe impacts requiring higher toughness properties. A study by Wen et al. [14] showed that the improved impact toughness by tempering might provide better wear resistance when steels are tested in severe impact loading conditions. Therefore, the balance of mechanical properties and wear resistance is essential when choosing the suitable steel for a given application. Fig. 12 shows the comparison of three tested steel variants (C43 WQ, C43 150 °C and C35) and their mechanical properties combined with the relative wear performance to the best performing steel (C43 WQ). Both of the shown steels (C43 and C35) can be used in water quenched or direct quenched state for good performance, but the low-temperature tempering of 150 °C shows even better combination of properties for the C43. Therefore, the final mechanical properties should be adjusted for the application by the parts manufacturer depending on the application and wear system. Similar performance review can be done also for the C43 300 °C and the C30, but the latter shows superior impact toughness with similar wear performance.

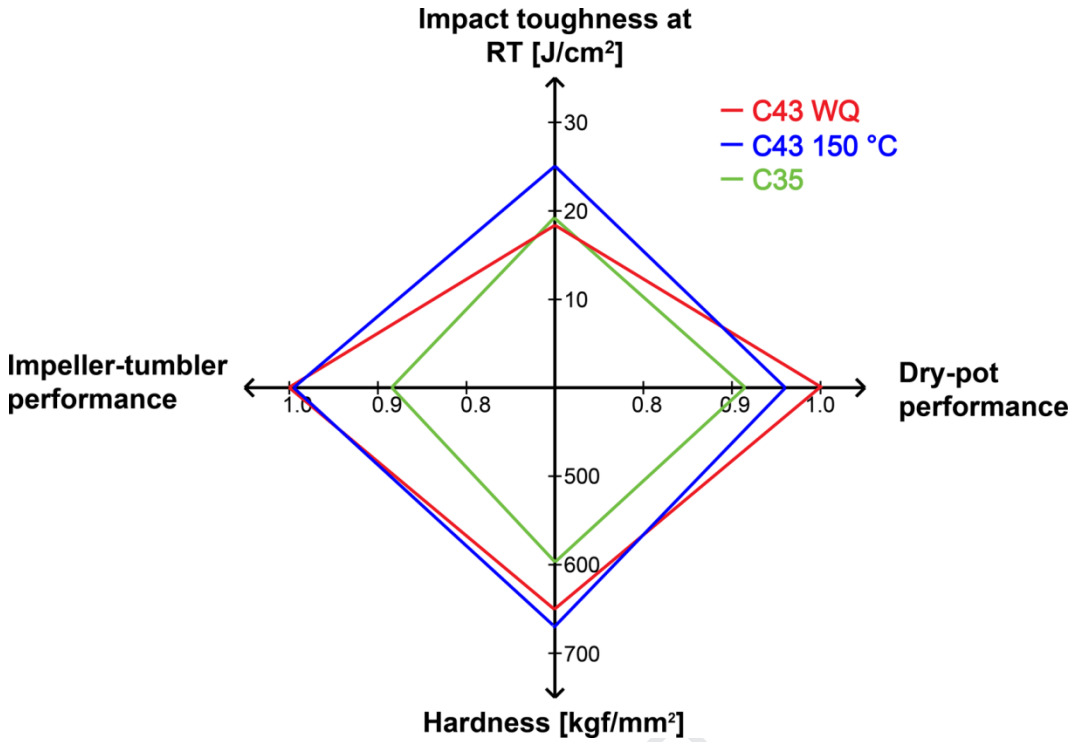


**Fig. 12.** Impact toughness, hardness and wear performance of C43 WQ, C43 150 °C and C35 compared. Wear performance calculated by relative mass loss to the best performing steel (C43 WQ).

Consequently, the emphasis should be on understanding the phenomena occurring on the surface layer when studying the wear resistance of steels. Work-hardening capability is one of the essential factors when testing for wear performance in impact-abrasive conditions [30,37,38]. Carbon-steels do not go as drastic work-hardening as some other steel grades or alloys, e.g. high-manganese steels, but the hardening of the steel surface is still considerable when subjected to heavy abrasion or impact wear. The differences in the work-hardening capability of the tested steels could explain part of the previously discussed minor differences in wear performance of similar hardness level steels. The work-hardening alone might not necessarily lead to better wear resistance, but the work-hardened surface layer should also be able to withstand surface fatigue, or in other words, the delamination effect of the hardened layer should be minimized. The ability to resist the removal of this highly deformed layer has a significant role in the wear performance of the steels [29,30,34]. The microhardness results indicate that the two direct-quenched steels (C30 and C35) with lower carbon content had more work-hardening capability in the current wear test conditions. Tempering in general decreases the strain-hardening capability of steel, but on the other hand, the increasing carbon content should increase the strain-hardening rate [7].

Retained austenite might improve the work-hardening capability of the steel as well, but in this study, it did not appear to have a clear effect on the wear resistance. The C43 WQ had more retained austenite present than the low-temperature tempered samples and better wear resistance. In contrast, the C43 200 °C had higher retained austenite content than the C35, but the latter had better performance in general. Hence, the retained austenite cannot be stated improving wear properties of the tested martensitic steels, as was also found in previous study with DQ&P steels [29].

Prior austenite grain size could also have an effect on the work-hardening of the steels. It is fairly known that the refining of grain size improves the strength of steels (Hall-Petch equation) and lowers the ductile-to-brittle transition temperature. However, the effect of grain size on the work-

hardening rate during impact or abrasive wear is quite unknown. In this study, the grain size was larger for the direct-quenched steels (C30 and C35) whereas the C43 had notably smaller grain size due to the austenitization. The steels with larger grain size had higher increase in the surface hardness. However, the DQ steels also had higher alloying element content compared to the fairly lean composition of the C43. Some elements, such as nickel, may also have an effect on work-hardening capability of steels during impact loading.

Though hardness was the main factor controlling impact-abrasive wear performance in the current study, more studies should be conducted in order to understand the effect of work-hardening and other factors, such as the prior austenite grain size and different alloying elements, on the wear resistance of martensitic steels. Consequently, the studied press-hardening steel (C43) proved to exhibit high mechanical properties and promising wear resistance in as-quenched and low-temperature tempered conditions. Therefore, the steel could be considered suitable for environments with harsh abrasive or impact-abrasive wear, such as wear-resistant material for different mining and mineral handling systems, or as blades for agricultural equipment.

## 4. SUMMARY AND CONCLUSIONS

In this study, a novel quench and press-hardening steel was inspected for wear performance in different quenched and tempered conditions. Mechanical properties were measured, and microstructural characterization was done in order to understand the effects of quenching and tempering. Wear testing was done with impeller-tumbler and dry-pot testing methods. The following conclusions were made:

(1) The C43 steel hardness exceeded 650HV/58 HRC in both water-quenched and low-temperature tempered (150 °C) conditions. High hardness, above 600 HV, was also achieved when tempered at 200 °C. Tempering at 300 and 400 °C decreased the hardness to levels of 500 and 400 HV, respectively. The highest tensile strength was achieved with the C43 WQ sample (2233 MPa) and the highest yield strength with the C43 200 °C (1616 MPa). Impact toughness properties increased with the low-temperature tempering treatments (150 and 200 °C).

(2) The initial hardness was the main factor controlling wear resistance in impeller-tumbler and dry-pot tests. Wear performance was measured by mass loss, and the increasing hardness resulted in decreased mass loss in the tested impact-abrasive and abrasive conditions. Differences in impact toughness properties, yield strength and uniform elongation did not show as strong correlation with the wear resistance as hardness did. The direct-quenched/water-quenched steel variants showed slightly better wear resistance when compared to the tempered variants at the same hardness level.

(3) Surface roughness and granite embedment generally followed the similar trend as the hardness and mass loss: steels with the highest hardness showed the lowest R-values and the least granite embedment. The impact-abrasive impeller-tumbler method produced higher surface roughness values compared to the more abrasive dry-pot.

(4) Wear surfaces showed greater depth of deformation for the impeller-tumbler tested samples. Increasing hardness decreased the depth of deformed microstructure and the penetration depth of the granite particles. More subsurface shear bands and cracks were discovered in the impeller-tumbler samples. Microhardness testing showed highest work-hardening of the worn surface for the direct-quenched samples.

ACKNOWLEDGEMENTS

This research has been done within the program Steel Ecosystem for Focused Applications (StEFA). We gratefully acknowledge financial support from Business Finland and the companies participating in the program. The corresponding author would also like to express his gratitude for the support provided by the University of Oulu Graduate School through the Advanced Materials Doctoral Program (ADMA-DP). Jenny and Antti Wihuri Foundation, Tauno Tönning Foundation and Walter Ahlström Foundation are also acknowledged for their financial support to the corresponding author.

REFERENCES

[1] R. Rementeria, I. García, M.M. Aranda, F.G. Caballero, Reciprocating-sliding wear behavior of nanostructured and ultra-fine high-silicon bainitic steels, Wear. 338–339 (2015) 202–209. doi:10.1016/j.wear.2015.06.011.

[2] E. Vuorinen, V. Heino, N. Ojala, O. Haiko, A. Hedayati, Erosive-abrasive wear behavior of carbide-free bainitic and boron steels compared in simulated field conditions, Proc. Inst. Mech. Eng. Part J J. Eng. Tribol. 232 (2018) 3–13. doi:10.1177/1350650117739125.

[3] E. Vuorinen, N. Ojala, V. Heino, C. Rau, C. Gahm, Erosive and abrasive wear performance of carbide free bainitic steels - Comparison of field and laboratory experiments, Tribol. Int. 98 (2016) 108–115. doi:10.1016/j.triboint.2016.02.015.

[4] B. Prakash, F.G. Caballero, R. Elvira, V. Smanio, T. Sourmail, C. Garcia-Mateo, et al., Wear of nano-structured carbide-free bainitic steels under dry rolling–sliding conditions, Wear. 298–299 (2012) 42–47. doi:10.1016/j.wear.2012.11.064.

[5] A.M. Gola, M. Ghadamgahi, S.W. Ooi, Microstructure evolution of carbide-free bainitic steels under abrasive wear conditions, Wear. 376–377 (2017) 975–982. doi:10.1016/j.wear.2016.12.038.

[6] M. Shah, S. Das Bakshi, Three-body abrasive wear of carbide-free bainite, martensite and bainite-martensite structure of similar hardness, Wear. 402–403 (2018) 207–215. doi:10.1016/j.wear.2018.02.020.

[7] G. Krauss, Martensite in steel: strength and structure, Mater. Sci. Eng. A. 273–275 (1999) 40–57. doi:10.1016/S0921-5093(99)00288-9.

[8] C. Ouchi, Development of Steel Plates by Intensive Use of TMCP and Direct, ISIJ Int. 41 (2001) 542–553. doi:10.2355/isijinternational.41.542.

[9] A.J. Kaijalainen, P.P. Suikkanen, T.J. Limnell, L.P. Karjalainen, J.I. Kömi, D.A. Porter, Effect of austenite grain structure on the strength and toughness of direct-quenched martensite, J. Alloys Compd. 577 (2013) S642–S648. doi:10.1016/j.jallcom.2012.03.030.

[10] A. Saastamoinen, A. Kaijalainen, J. Heikkala, D. Porter, P. Suikkanen, The effect of tempering temperature on microstructure, mechanical properties and bendability of direct-quenched low-alloy strip steel, Mater. Sci. Eng. A. 730 (2018) 284–294. doi:10.1016/j.msea.2018.06.014.

[11] G. Krauss, Tempering of martensite in carbon steels, in: Phase Transform. Steels Vol. 2 Diffus. Transform. High Strength Steels, Model. Adv. Anal. Tech., Woodhead Publishing Limited, 2012: pp. 126–150. doi:10.1533/9780857096111.1.126.

[12] H.K.D.H. Bhadeshia, R. Honeycombe, The Tempering of Martensite, in: Steels Microstruct. Prop., Third Edit, 2006: pp. 183–208. doi:https://doi.org/10.1016/B978-075068084-4/50011-

X.
[13] C. Trevisiol, A. Jourani, S. Bouvier, Effect of hardness, microstructure, normal load and abrasive size on friction and on wear behaviour of 35NCD16 steel, Wear. 388–389 (2017) 101–111. doi:10.1016/j.wear.2017.05.008.
[14] E. Wen, R. Song, W. Xiong, Effect of Tempering Temperature on Microstructures and Wear Behavior of a 500 HB Grade Wear-Resistant Steel, Metals (Basel). 9 (2019) 45. doi:10.3390/met9010045.
[15] M.X. Wei, S.Q. Wang, L. Wang, X.H. Cui, K.M. Chen, Effect of tempering conditions on wear resistance in various wear mechanisms of H13 steel, Tribol. Int. 44 (2011) 898–905. doi:10.1016/j.triboint.2011.03.005.
[16] O. Seppälä, S. Uusikallio, J. Larkiola, A tool for computer-aided calculation of grain size, in: D. Szeliga, L. Rauch (Eds.), B. Abstr. XXVI Int. Conf. Comput. Methods Mater. Technol. KomPlasTech 2019, ISBN: 978-83-947091-4-3, 2019: pp. 128–130. http://www.aknet.biz.pl/.
[17] R. Higginson, M. Sellars, Worked Examples in Quantitative Metallography, 1. Edition, CRC Press, 2003.
[18] V. Ratia, K. Valtonen, A. Kemppainen, V.-T. Kuokkala, High-stress abrasion and impact-abrasion testing of wear resistant steels, Tribol. Online. 8 (2013) 152–161. doi:10.2474/trol.8.152.
[19] N. Ojala, K. Valtonen, P. Kivikytö-Reponen, P. Vuorinen, P. Siitonen, V.-T. Kuokkala, Effect of test parameters on large particle high speed slurry erosion testing, Tribol. - Mater. Surfaces Interfaces. 8 (2014) 98–104. doi:10.1179/1751584X14Y.0000000066.
[20] N. Ojala, K. Valtonen, A. Antikainen, A. Kemppainen, J. Minkkinen, O. Oja, et al., Wear performance of quenched wear resistant steels in abrasive slurry erosion, Wear. 354–355 (2016) 21–31. doi:10.1016/j.wear.2016.02.019.
[21] N. Ojala, K. Valtonen, J. Minkkinen, V.T. Kuokkala, Edge and particle embedment effects in low- and high-stress slurry erosion wear of steels and elastomers, Wear. 388–389 (2017) 126–135. doi:10.1016/j.wear.2017.06.004.
[22] K. Valtonen, V. Ratia, N. Ojala, V.-T. Kuokkala, Comparison of laboratory wear test results with the in-service performance of cutting edges of loader buckets, Wear. 388–389 (2017) 93–100. doi:10.1016/j.wear.2017.06.005.
[23] K. Valtonen, K. Keltamäki, V.T. Kuokkala, High-stress abrasion of wear resistant steels in the cutting edges of loader buckets, Tribol. Int. 119 (2018) 707–720. doi:10.1016/j.triboint.2017.12.013.
[24] B. Hutchinson, D. Lindell, M. Barnett, Yielding Behaviour of Martensite in Steel, ISIJ Int. 55 (2015) 1114–1122. doi:10.2355/isijinternational.55.1114.
[25] B. Hutchinson, P. Bate, D. Lindell, A. Malik, M. Barnett, P. Lynch, Plastic yielding in lath martensites – An alternative viewpoint, Acta Mater. 152 (2018) 239–247. doi:10.1016/j.actamat.2018.04.039.
[26] R.M. Horn, R.O. Ritchie, Mechanisms of tempered martensite embrittlement in medium-carbon steels, Metall. Trans. A. 9 (1978) 1039–1053. doi:https://doi.org/10.1007/BF02652208.
[27] G. Krauss, Low toughness and embrittlement phenomena in steels, in: Steels Process. Struct. Perform., Second Edi, ASM International, 2015: pp. 439–485.
[28] O. Haiko, I. Miettunen, D. Porter, N. Ojala, V. Ratia, V. Heino, et al., Effect of Finish Rolling and Quench Stop Temperatures on Impact-Abrasive Wear Properties of 0.35 % Carbon Direct-Quenched Steel, Tribol. - Finnish J. Tribol. 35 (2017) 5–21. https://journal.fi/tribologia/article/view/59344.
[29] O. Haiko, M. Somani, D. Porter, P. Kantanen, J. Kömi, N. Ojala, et al., Comparison of impact-abrasive wear characteristics and performance of direct quenched (DQ) and direct

quenched and partitioned (DQ&P) steels, Wear. 400–401 (2018) 21–30. doi:10.1016/j.wear.2017.12.016.

[30] N. Ojala, K. Valtonen, V. Heino, M. Kallio, J. Aaltonen, P. Siitonen, et al., Effects of composition and microstructure on the abrasive wear performance of quenched wear resistant steels, Wear. 317 (2014) 225–232. doi:10.1016/j.wear.2014.06.003.

[31] V. Ratia, I. Miettunen, V.T. Kuokkala, Surface deformation of steels in impact-abrasion: The effect of sample angle and test duration, Wear. 301 (2013) 94–101. doi:10.1016/j.wear.2013.01.006.

[32] R.. Wilson, J.. Hawk, Impeller wear impact-abrasive wear test, Wear. 225 (1999) 1248–1257. doi:10.1016/S0043-1648(99)00046-0.

[33] K. Valtonen, N. Ojala, O. Haiko, V. Kuokkala, Comparison of various high-stress wear conditions and wear performance of martensitic steels, Wear. 426–427 (2019) 3–13. doi:10.1016/j.wear.2018.12.006.

[34] V. Ratia, K. Valtonen, A. Kemppainen, V.-T. Kuokkala, The Role of Edge-Concentrated Wear in Impact-Abrasion Testing, Tribol. Online. 11 (2016) 410–416. doi:10.2474/trol.11.410.

[35] Y. Xu, J. Zhang, Y. Bai, M.A. Meyers, Shear localization in dynamic deformation: Microstructural evolution, Metall. Mater. Trans. A Phys. Metall. Mater. Sci. 39 A (2008) 811–843. doi:10.1007/s11661-007-9431-z.

[36] Y.Y. Yang, H.S. Fang, Y.K. Zheng, Z.G. Yang, Z.L. Jiang, The failure models induced by white layers during impact wear, Wear. 185 (1995) 17–22. doi:10.1016/0043-1648(94)06586-1.

[37] M. Lindroos, V. Ratia, M. Apostol, K. Valtonen, A. Laukkanen, W. Molnar, et al., The effect of impact conditions on the wear and deformation behavior of wear resistant steels, Wear. 328–329 (2015) 197–205. doi:10.1016/j.wear.2015.02.032.

[38] J. Rendón, M. Olsson, Abrasive wear resistance of some commercial abrasion resistant steels evaluated by laboratory test methods, 267 (2009) 2055–2061. doi:10.1016/j.wear.2009.08.005.

Highlights

- Medium carbon (0.4C) press-hardening steel was tempered at different temperatures.
- Yield strength and impact toughness were improved by tempering.
- Wear resistance was found to correlate with the initial hardness.
- Direct-quenched steels showed slightly lower mass loss than tempered steels.

**Declaration of interests**

☒ The authors declare that they have no known competing financial interests or personal relationships that could have appeared to influence the work reported in this paper.

☐The authors declare the following financial interests/personal relationships which may be considered as potential competing interests: